Journal of Biomedical Optics

BiomedicalOptics.SPIEDigitalLibrary.org

Ex vivo characterization of normal and adenocarcinoma colon samples by Mueller matrix polarimetry

Iftikhar Ahmad
Manzoor Ahmad
Karim Khan
Sumara Ashraf
Shakil Ahmad
Masroor Ikram

SPIE.

Ex vivo characterization of normal and adenocarcinoma colon samples by Mueller matrix polarimetry

Iftikhar Ahmad,[a,b,*] Manzoor Ahmad,[a,c] Karim Khan,[a] Sumara Ashraf,[a] Shakil Ahmad,[d] and Masroor Ikram[a]
[a]Pakistan Institute of Engineering and Applied Sciences, Department of Physics and Applied Mathematics, Nilore, Islamabad 45650, Pakistan
[b]Center for Nuclear Medicine and Radiotherapy (CENAR), Brewery Road, 17, Quetta, Pakistan
[c]Islamia College (University), Department of Physics, Peshawar, Pakistan
[d]Swat Institute of Nuclear Medicine, Oncology and Radiotherapy (SINOR), Saidu Sharif, 50, Swat, Pakistan

Abstract. Mueller matrix polarimetry along with polar decomposition algorithm was employed for the characterization of *ex vivo* normal and adenocarcinoma human colon tissues by polarized light in the visible spectral range (425–725 nm). Six derived polarization metrics [total diattenuation (D_T), retardance (R_T), depolarization (Δ_T), linear diattenuation (D_L), retardance (δ), and depolarization (Δ_L)] were compared for normal and adenocarcinoma colon tissue samples. The results show that all six polarimetric properties for adenocarcinoma samples were significantly higher as compared to the normal samples for all wavelengths. The Wilcoxon rank sum test illustrated that total retardance is a good candidate for the discrimination of normal and adenocarcinoma colon samples. Support vector machine classification for normal and adenocarcinoma based on the four polarization properties spectra (Δ_T, Δ_L, R_T,and δ) yielded 100% accuracy, sensitivity, and specificity, while both D_T and D_L showed 66.6%, 33.3%, and 83.3% accuracy, sensitivity, and specificity, respectively. The combination of polarization analysis and given classification methods provides a framework to distinguish the normal and cancerous tissues. [DOI: 10.1117/1.JBO.20.5.056012]

Keywords: Mueller matrix polarimetry; adenocarcinoma colon; polar decomposition.

Paper 140811R received Dec. 8, 2014; accepted for publication May 4, 2015; published online May 28, 2015.

1 Introduction

Precancerous polyps initiate the majority of colon cancer,[1] which is one of the major causes of cancer-related deaths.[2] The detection of such precancerous polyps at an early stage, followed by surgical removal during colonoscopy, can greatly enhance the survival rates and patient's quality of life. However, the diagnosis of precancerous polyps at early stage by white light colonoscopy is very challenging.[3] Polypectomy is still considered to be a standard diagnostic technique for colon cancer, which has its own set of shortcomings. In this technique, excision of a polyp for biopsy followed by histopathology needs extensive examination of biopsy samples by microscope for several morphological changes (such as nuclear and cellular enlargement, increased variation in nuclear size and shape, and increased concentration of chromatin[4]) that occur during the development of cancer in the polyp. Therefore, the performance of polypectomy is greatly dependent on the expertise of the surgeon/pathologist besides its noninvasive nature. Moreover, the excision of multi polyps and their histopathology along with identification of clear circumferential margins during surgery for colon cancer further complicate this procedure. Therefore, it demands a noninvasive automated modality to overcome the above mentioned issues.

Polarized light for cancer diagnosis is gathering increased interest due to frequently observed contrasts in polarization parameters between normal and malignant tissues. It has great advantages compared to other optical techniques in signal strength and sensitivity to cellular structures, and thus conveys rich morphological and functional information about the biological tissue. Many studies implementing polarimetric contrasts in various biomedical fields such as dermatology, ophthalmology, gynecology, etc., have already been carried out. Various dermatological diseases such as lupus lesions and malignant moles are identified by polarimetric measurement.[5,6] Jacques et al. reported that surgical excision of skin cancers can be guided using polarized light and developed a handheld polarization camera for this purpose.[7] Polarization images of precancerousoral tissues in hamster cheek pouches showed considerable differences in depolarization and retardance images between normal and precancerous tissues.[8] Polarized light has been used for extraction of quantitative information about the size of cell nuclei from imaging the human epithelial tissue.[4] Shukla and Pradhan showed that depolarization power is sensitive to morphological changes in the normal and dysplastic states of epithelial cervical tissue.[9] Contrast in polarization properties such as retardance, diattenuation, and depolarization has been observed for hepatic tissue,[10] connective tissue,[11] cervical precancer,[12] myocardium samples,[13] and gastric tissues.[14] Pierangelo et al. have correlated various histological variants of human colon tumor to depolarization using multispectral Mueller matrix polarimetry.[15,16] Robust statistical analysis along with suitable classification of healthy and cancerous colon tissues in conjunction with the Mueller matrix polarimetry technique is of

*Address all correspondence to: Iftikhar Ahmad, E-mail: iahmadmp@gmail.com

1083-3668/2015/$25.00 © 2015 SPIE

paramount importance for implementation of the technique at the clinical level. Mueller matrix polarimetry is not exhausted much with suitable statistical analysis, particularly the studies conducted by Pierangelo et al. for colon cancer detection.

In this study, we have investigated the relative contrasts of polarization properties (retardance, diattenuation, and depolarization) for *ex vivo* normal and adenocarcinoma human colon tissue samples using Mueller matrix polarimetry in the complete visible spectral region (425–725 nm). For statistical analysis, Wilcoxon rank sum was employed for the selection of suitable polarimetric metrics for the classification of normal and adenocarcinoma colon samples. We have used a support vector machine (SVM) for classification of our data, and discussed the sensitivity and specificity in detail. The results may have important biomedical applications, specifically in the automated noninvasive diagnosis of cancer.

2 Materials and Methods

2.1 *Microscopic Structure of Colon Tissue*

In this study, we have compared the polarimetric properties of adenocarcinoma and normal colon tissues. Colon tissue is composed of three main layers: mucosa, submucosa, and muscularispropria[17,18] that can be clearly seen in the microscopic image of a normal colon tissue as shown in Fig. 1. Mucosa can be further divided into: (a) the superficial one cell thick epithelium layer; (b) the lamina propria, which is composed of a loose network of collagen fibers and blood capillaries; and (c) the muscularis mucosa, which is a thin layer of smooth muscles and separates mucosa from submucosa. Submucosa contains a dense network of collagen fibers, blood vessels, and lymphatic vessels but no glands are present. Muscularis propria is composed of muscular tissue and separates submucosa from serosa, which is the inner lipid layer and contains cells that produce lubricating fluid for friction reduction.[19] Sometimes serosa is termed as the fourth layer of colon tissue.

Approximately 90%–95% of malignant tumors of the colorectal system are derived from epithelial cells, usually in the large intestine.[20] Adenocarcinomas are derived from the glandular epithelium. The main characteristic of adenocarcinoma tissue is the significant nuclear enlargement compared to normal tissue as observed in both light scattering spectroscopy and morphometric measurements.[19]

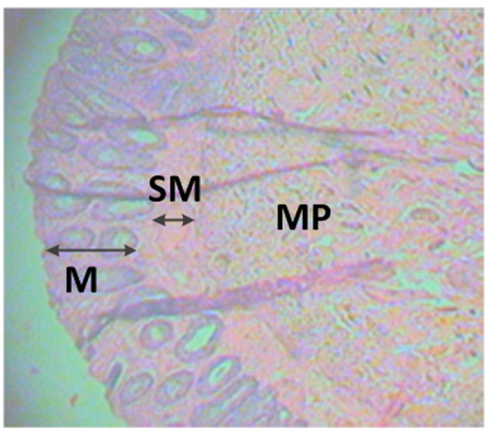

Fig. 1 Microscopic image of normal colon tissue sample with 20× objective lens showing its different layers: the mucosa (M), the submucosa (SM), and muscularis propria (MP).

2.2 *Sample Preparation*

A total of 24 colon tissue samples obtained from 24 different patients were examined in this study. Samples were categorized into two classes, one having 16 adenocarcinoma colon tissue samples and the other with 8 normal colon tissue samples. These tissue samples were either removed by biopsy or partial colectomy. Each tissue sample was fixed in formalin, embedded in paraffin and sliced in 3-μm thick sections using Leica microtome. These tissue samples were fixed on glass slides, stained with hematoxylin and eosin (H&E) and covered with a glass coverslip. Polarimetric analysis was sequentially performed on same tissue slides after their pathological evaluation.

2.3 *Mueller Matrix Polarimeter*

In this study, we have used a computer-controlled Mueller matrix spectro-polarimetery system (Axometrics, Huntsville, Alabama; schematic is shown in Fig. 2). A low-noise xenon lamp (150 W) is used as the input light source. Any wavelength in the range of 400–800 nm can be selected with a built-in diffraction grating monochromator with an accuracy of ± 0.5 nm. The light source is coupled to the polarization state generator (PSG) via fiber-optic cable. PSG generates various desired polarization states for sample illumination. The beam illumination diameter was 6 mm at the sample. After interacting with the sample the light is passed through a polarization state analyzer (PSA) which is connected to a computer.

All samples were illuminated with four different input polarization states with a beam diameter of 6 mm. An average of three measurements for each tissue sample was considered to minimize the experimental fluctuation. The input polarization states include horizontal polarization ($\mathrm{H}:[1100]^{\mathrm{T}}$), vertical polarization ($\mathrm{V}:[1-100]^{\mathrm{T}}$), linear +45 deg polarization ($\mathrm{P}:[1010]^{\mathrm{T}}$), and right circular polarization ($\mathrm{R}:[1001]^{\mathrm{T}}$). After interaction with the sample, each polarization state was analyzed on four different polarization states. Thus, a total of 16 combinations were obtained. These include: HH, HV, HP, HR, VH, VV, VP, VR, PH, PV, PP, PR, RH, RV, RP, and RR, in which the first letters indicate the polarization states of the PSG, while the second letter indicates the polarization state analyzed by PSA. For example, "HV" means the incident polarization state is horizontal ($\mathrm{H}:[1100]^{\mathrm{T}}$), which is analyzed onto vertical polarized light($\mathrm{V}:[1-100]^{\mathrm{T}}$). A Mueller matrix was constructed using these 16 raw measurements.[10]

2.4 *Polar Decomposition*

The input Stokes vector S_i is changed to the output Stokes vector S_0 by polarization transfer function of the sample which can be written mathematically as $S_0 = \mathbf{M}\, S_i$, where M is the 4×4 Mueller matrix. The Mueller matrix contains the complete polarimetric fingerprints of the sample in "lumped" form. Various decomposition methods are used to individually retrieve these polarimetric properties. Polar decomposition[21] is widely used in tissue polarimetry and is briefly discussed below.

The Mueller matrix of the sample can be expressed as the product of three basis matrices describing the three basic medium polarization properties as given below:

$$M = M_{\Delta} M_R M_D,$$

where M_{Δ} is the depolarization matrix, M_R is the retardance matrix, and M_D is the diattenuation matrix. The derived

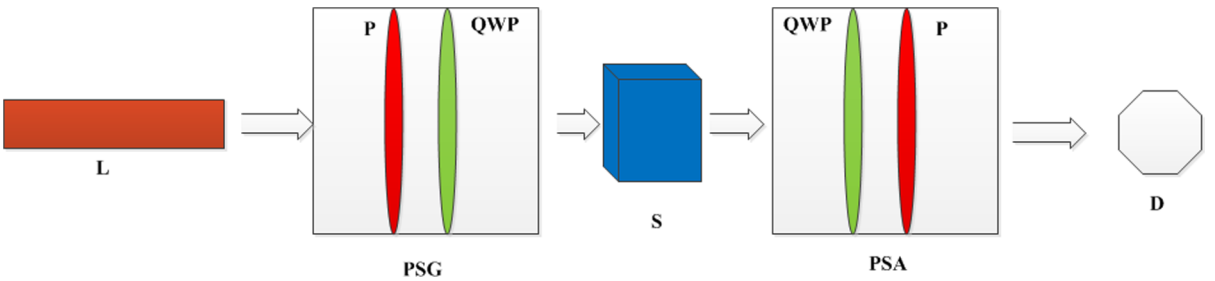

Fig. 2 Schematic diagram of Mueller matrix polarimeter consists of light source (L), polarization state generator (PSG), sample (S), polarization state analyzer (PSA), and detector (D).

polarization parameters are expected to be influenced by the choice of the basis matrices' ordering due to the noncommuting nature of matrix multiplication.[22] However, recent studies have shown that such ambiguity can be exclusively minimal under certain conditions such as very thin samples where multiple scattering is exceedingly negligible.[23]

The total depolarization Δ_T and linear depolarization Δ_L are calculated from the depolarization matrix M_Δ, as given

$$\Delta_T = 1 - \frac{|\mathrm{tr}(m_\Delta)|}{3}, \quad \Delta_L = 1 - \frac{|m_\Delta(1,1) + m_\Delta(2,2)|}{2},$$

where "tr" represents "trace" and m_Δ is a 3×3 submatrix formed by omitting the first row and column of the full matrix M_Δ

The retardance matrix M_R is decoupled to calculate the total retardance R and linear retardance δ, as given

$$R_T = \cos^{-1}\left[\frac{\mathrm{tr}(M_R)}{2} - 1\right],$$

$$\delta = \cos^{-1} \times \left[\sqrt{\{M_R(2,2) + M_R(3,3)\}^2 + \{M_R(3,2) - M_R(2,3)\}^2} - 1\right].$$

Total diattenuation D_T and linear diattenuation D_L are calculated from the first row of the experimental Mueller matrix as

$$D_T = \frac{1}{m_{11}}\sqrt{m_{12}^2 + m_{13}^2 + m_{14}^2}, \quad D_L = \frac{1}{m_{11}}\sqrt{m_{12}^2 + m_{13}^2}.$$

Further details on polar decomposition can be found in the literature.[8,24]

2.5 *Statistical Analysis*

Tissue samples were divided into normal and cancerous groups based on histopathological reports. The nonparametric Wilcoxon rank-sum test was utilized to compare various polarimetric properties of the two groups with a significance level of 0.05. An SVM algorithm was employed for classification of the samples on the basis of contrast in the polarimetric properties.[25] Statistical parameters such as accuracy, sensitivity, specificity, Mathew correlation coefficient, and F-measure were calculated from SVM. All data processing and statistical data analysis was performed using MATLAB®.

3 Results and Discussion

First, the experimental system is validated in the wavelength range of 400–800 nm (25-nm step size) for the standard samples (linear polarizer and retarder; quarter wave plate (QWP) at 632.8 nm) of known polarization properties. The Mueller matrix for each sample was measured and then decomposed via a polar decomposition method and corresponding polarization properties were extracted. Linear retardance of a retarder is presented in Fig. 3(a), while linear diattenuation of the polarizer is shown

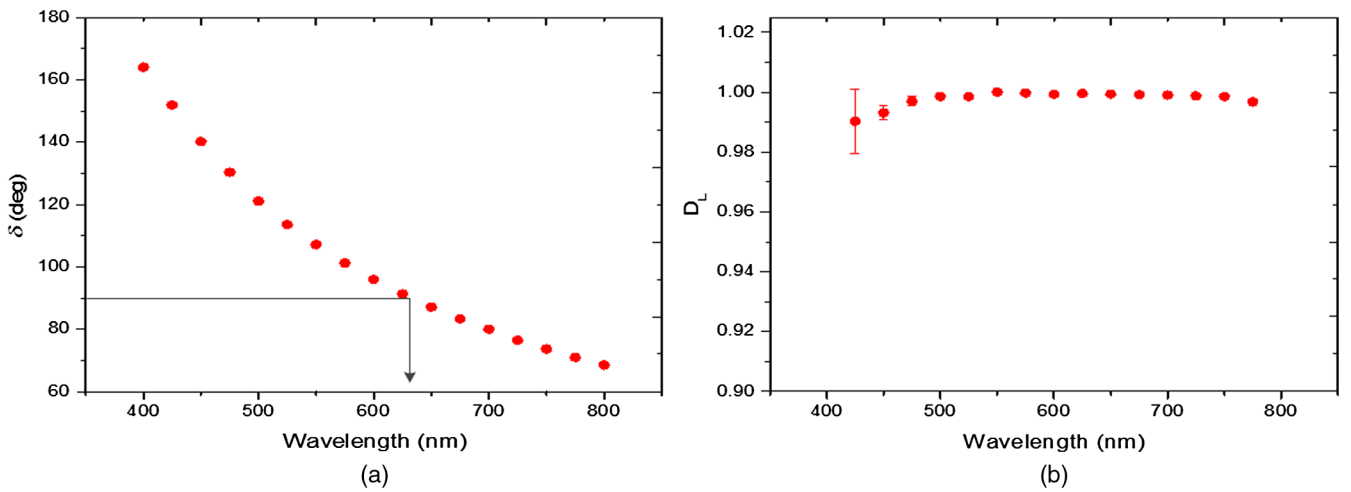

Fig. 3 (a) Linear retardance of retarder [quarter-wave plate (QWP) at 632.8 nm as indicated] and linear diattenuation of polarizer (b) in the spectral range from 400 to 800 nm.

in Fig. 3(b). Analyses of Fig. 3 demonstrate that the error in both D_L and δ reduces with wavelength. A maximum of 1.1% error exists in the calculation of both linear diattenuation and retardance as shown in Fig. 3. It may be noted that the error bars for linear retardance are smaller than the symbols used in Fig. 3(b) and are, therefore, not visible. The small error and almost no fluctuations in the standard samples of retarder that behave as QWP at 632.8 nm [indicated in Fig. 3(a)] and linear polarizer validate the excellent performance of the Mueller matrix polarimetric system and decomposition algorithms.

Comparison of total and linear depolarization for normal and adenocarcinoma colon samples at seven different wavelengths (425–725 nm) is illustrated in Fig. 4. Each numerical value of the polarimetric parameter shown in Fig. 4 (and subsequent figures) corresponds to the average value taken over all samples belonging to normal and cancerous groups. It is noted that both total and linear depolarizations are significantly higher for adenocarcinoma samples as compared to normal colon tissue samples at all investigated wavelengths. Furthermore, no overlap in the error bars between cancerous and normal samples was observed. Significant contrast in depolarization suggests that it can be exploited for discriminating adenocarcinoma from normal tissue samples. Linear depolarization has values similar to the total depolarization values over the entire spectral range. This indicates that linear depolarization is the main contributor of total depolarization for both cancerous and normal tissue samples.

The observed contrast in depolarization can be correlated to the morphological changes that occur at histological and molecular levels in the transition from the normal to malignant phase of tissue. The distortion of normal microarchitecture in cancerous tissue samples can be easily seen from the comparison of colon tissue images shown in Fig. (5). Contrary to normal tissue [Fig. 5(a)], the carcinoma tissues have malignant glands of variable sizes, nuclear stratification of the cells lining the glands [Fig. 5(b)] and disorganized fibrous stroma Fig. 5(c). The increase in depolarization for cancerous tissue samples can be correlated to these alterations as reported in other studies.[26–29]

Figure 6 depicts the total and linear retardance, while Fig. 7 shows the total and linear diattenuation for normal and adenocarcinoma tissue samples. It can be noted that both retardance and diattenuation are higher for carcinoma tissues as compared to normal tissues. However, the contrast in retardance for both groups is considerably higher than diattenuation. Retardation of polarized light in biological tissues is primarily attributed to the optical anisotropy of the collagen fibers. The network of these fibers is disturbed in the malignant colorectal tissue[30] as illustrated in Fig. 5. Boosted collagen metabolism[31] and enhanced collagen density in colon adenocarcinoma have been observed

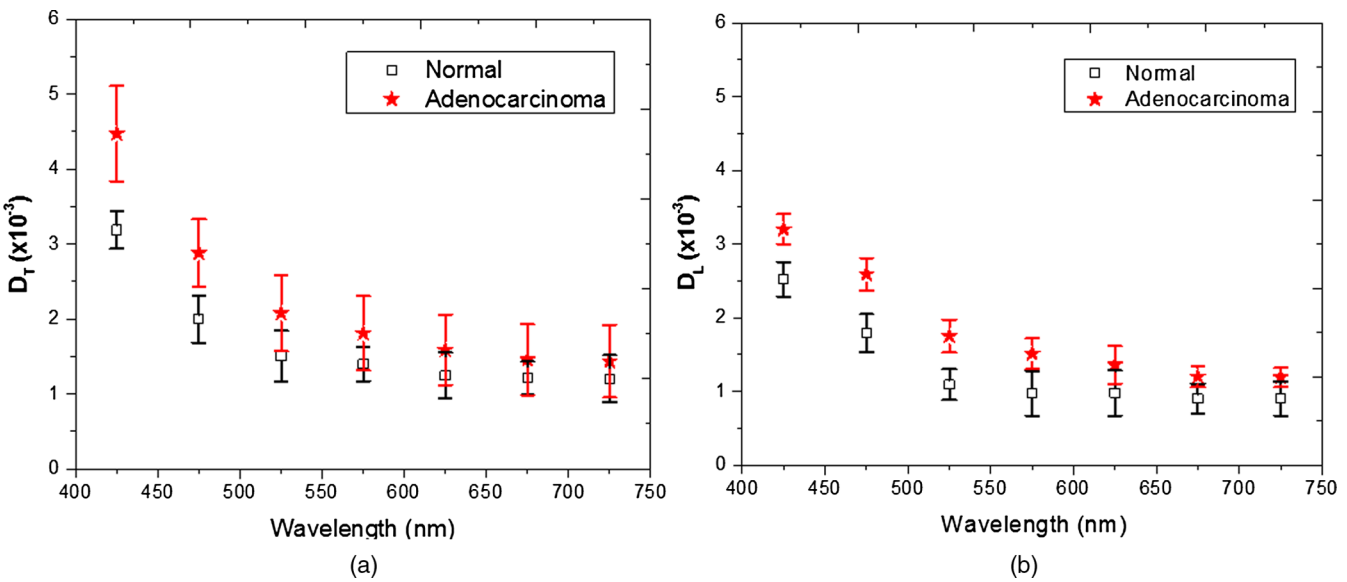

Fig. 4 Total (a) and linear (b) depolarization comparison for normal (rectangle) and adenocarcinoma (star) colon samples at different wavelengths (425–725 nm).

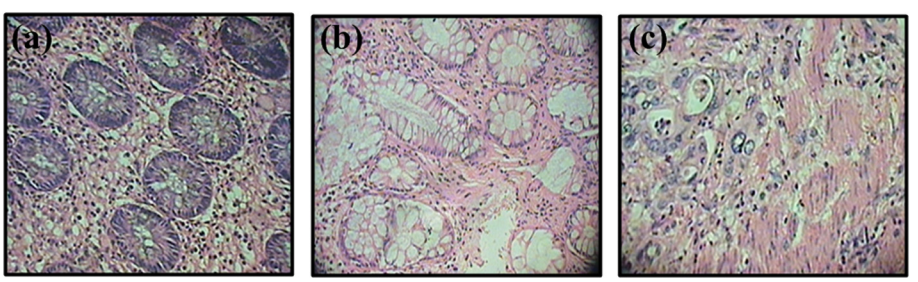

Fig. 5 Images of 3-μm thick normal (a) and cancerous (b and c) colon tissues with 40× objective lens. Malignant glands of variable sizes and disorganized fibrous stroma in (b and c) can be seen.

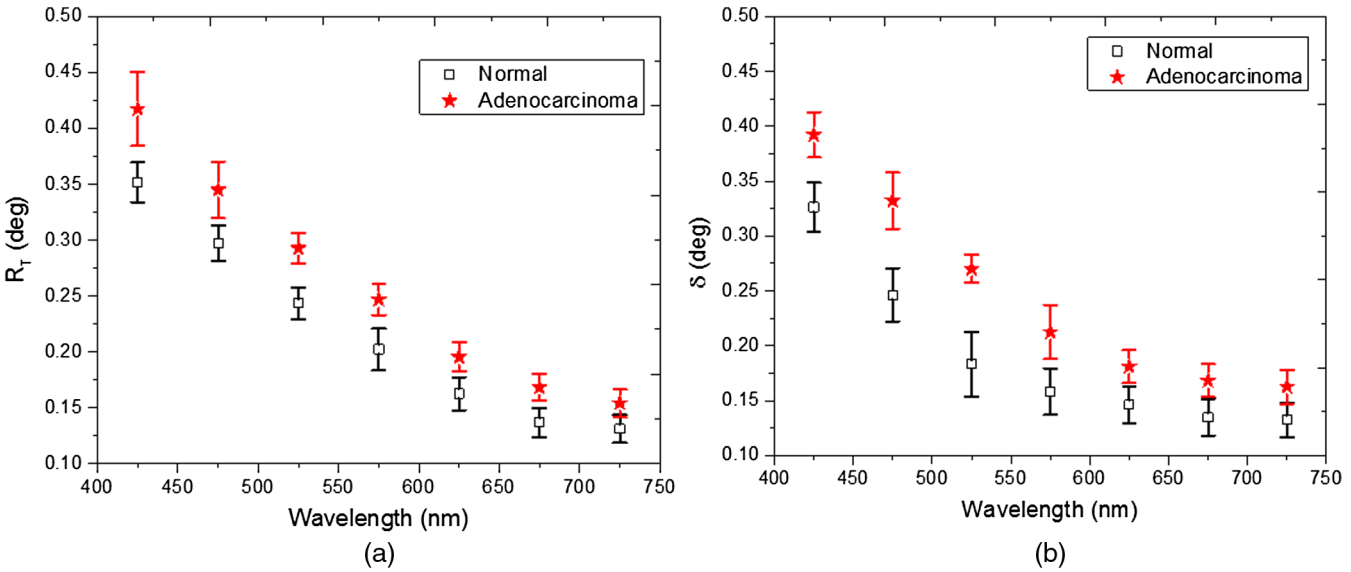

Fig. 6 Total (a) and linear (b) retardance for normal (rectangle) and carcinoma (star) tissues in the spectral range (425–725 nm).

by electron microscopy,[32] which amplifies the retardance of such tissues.

The positions of the average output Stoke vectors of linearly (H, V, P, R) and circularly (RC, LC) polarized light have been compared for both normal and cancerous tissue groups. The results, shown in Fig. 8, provide a quantitative fingerprint of the contrast in the polarimetric parameters of both groups.

Table 1 illustrates a typical comparison between an experimental Mueller matrix and the decomposed diattenuation M_D, retardance M_R and depolarization M_Δ basis matrices for adenocarcinoma and normal colon samples at 425 nm. The diagonal elements of the Mueller matrices are significantly higher than the off diagonal elements indicating the high depolarization nature of colon tissue samples. It is interesting to note that an identical relation between the diagonal elements of the Mueller matrix is followed by both adenocarcinoma and normal colon tissues, i.e.,

$$M_{22} = M_{33} > M_{44}$$

for both types of samples. This is typical of the Rayleigh scattering regime, where the circularly polarized incident light is depolarized faster than linearly polarized incident light. Further, in turbid media such as biological tissues, the depolarization of incident linearly polarized light is primarily caused by randomization of the field vector's direction due to scattering. Therefore, we believe that the linear depolarization in such a situation will be the same for any orientation of the incident linear polarization vector resulting in $M_{22} = M_{33}$.[33] The same trend is observed in other studies for various tissues.[15,19,34]

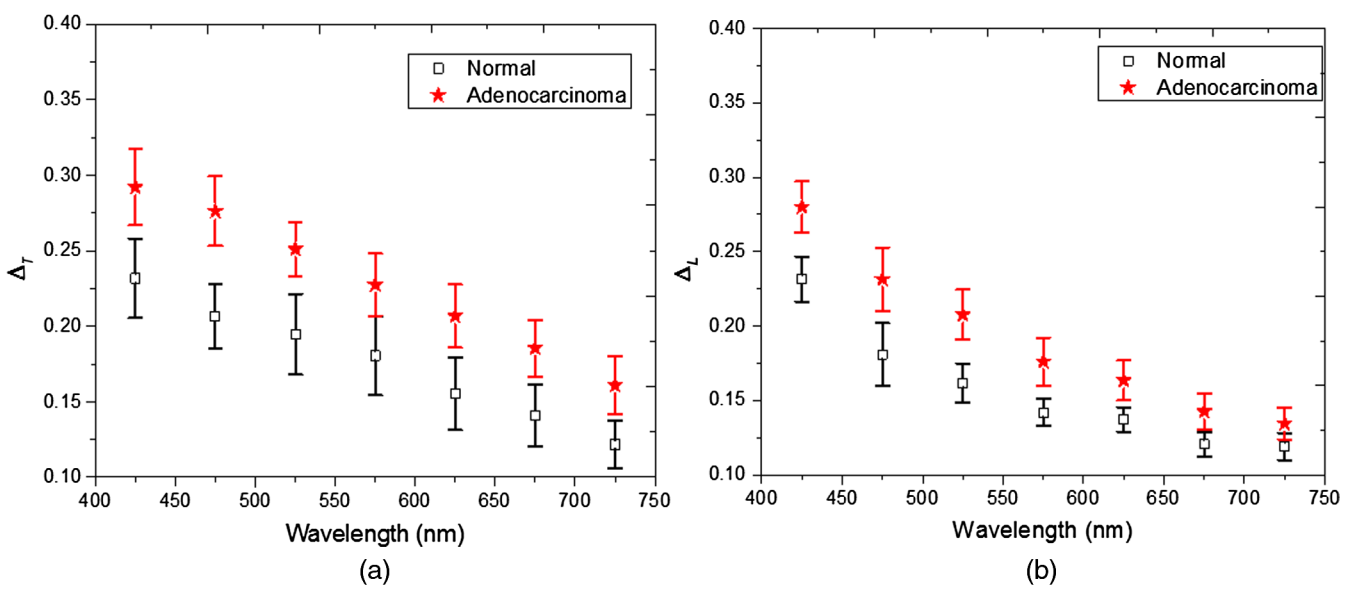

Fig. 7 Total (a) and linear (b) diattenuation for normal (rectangle) and carcinoma (star) tissues against wavelength.

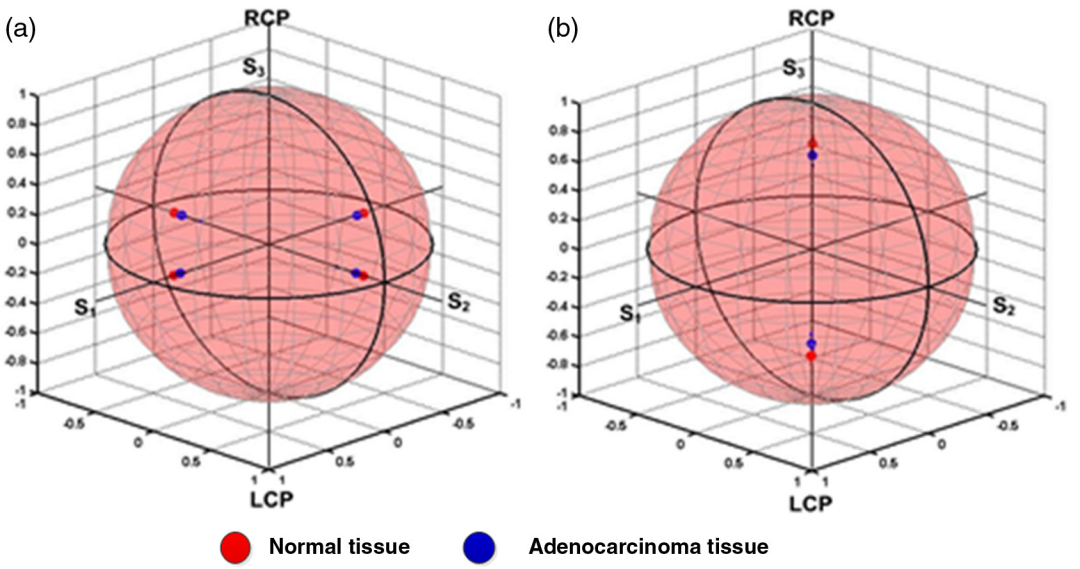

Fig. 8 Comparison of positions of average output Stokes vector of linearly (a) and circularly (b) polarized light on Poincare sphere for normal and adenocarcinoma tissues.

In order to assess the performance of the above mentioned polarization method to differentiate normal and adenocarcinoma colon tissue samples, we have employed the Wilcoxon rank sum test and SVM for classification.[35] We have performed the Wilcoxon rank sum test and SVM over all the six measured polarization properties of each individual sample and over each wavelength.

Figure 9 demonstrates the p values obtained by the Wilcoxon test for six polarimetric properties at different wavelengths with a significance level of $p \leq 0.05$. Polarization properties with $p \leq 0.05$ can be utilized for discrimination of normal and adenocarcinoma colon samples with higher than 95% confidence level. From Fig. 9, we conclude that depolarization and retardance are good candidates for the discrimination of normal and adenocarcinoma colon samples.

We have employed SVM classifier for further investigation to confirm the capability of the measured polarization metrics for classification of normal and adenocarcinoma colon samples. Different performance parameters including test accuracy, sensitivity, specificity, Mathew's correlation coefficient (MCC), and F-measure were used to evaluate the performance of SVM. SVM was individually applied over the spectrum of six polarization properties and also with different combinations of these properties for all 24 samples. Table 2 shows that SVM classified the interrogated polarization properties very well except for total and linear diattenuations. From Table 2, it can be noted that

Table 1 Comparison of experimental Mueller matrix and its decomposed basis matrices for cancerous and normal tissues at 425 nm.

	Adenocarcinoma sample	Normal sample
M	$\begin{bmatrix} 1 & 0.003 & 0 & -0.004 \\ 0 & 0.722 & 0.002 & -0.004 \\ -0.001 & 0.004 & 0.722 & 0.001 \\ 0.001 & 0.006 & -0.001 & 0.669 \end{bmatrix}$	$\begin{bmatrix} 1 & 0.003 & -0.002 & -0.002 \\ -0.003 & 0.761 & 0.002 & 0.002 \\ 0.002 & 0.003 & 0.762 & -0.002 \\ -0.003 & -0.008 & -0.002 & 0.738 \end{bmatrix}$
M_D	$\begin{bmatrix} 1 & 0.003 & 0 & -0.004 \\ 0.003 & 0.999 & 0 & 0 \\ 0 & 0 & 0.999 & 0 \\ 0.004 & 0 & 0 & 0.999 \end{bmatrix}$	$\begin{bmatrix} 1 & 0.002 & -0.002 & -0.002 \\ 0.002 & 0.999 & 0 & 0 \\ -0.002 & 0 & 0.999 & 0 \\ 0.002 & 0 & 0 & 0.999 \end{bmatrix}$
M_R	$\begin{bmatrix} 1 & 0 & 0 & 0 \\ 0 & 0.999 & -0.002 & -0.007 \\ 0 & 0.002 & 0.999 & 0.002 \\ 0 & 0.007 & -0.002 & 0.999 \end{bmatrix}$	$\begin{bmatrix} 1 & 0 & 0 & 0 \\ 0 & 0.999 & 0 & 0.006 \\ 0 & 0 & 0.999 & 0 \\ 0 & -0.006 & 0 & 0.999 \end{bmatrix}$
M_Δ	$\begin{bmatrix} 1 & 0 & 0 & 0 \\ -0.002 & 0.722 & -0.003 & -0.001 \\ -0.001 & 0.003 & 0.722 & 0 \\ 0.003 & 0.001 & 0 & 0.669 \end{bmatrix}$	$\begin{bmatrix} 1 & 0 & 0 & 0 \\ -0.005 & 0.761 & 0.002 & -0.003 \\ 0.003 & 0.002 & 0.761 & -0.002 \\ -0.001 & -0.003 & -0.002 & 0.737 \end{bmatrix}$

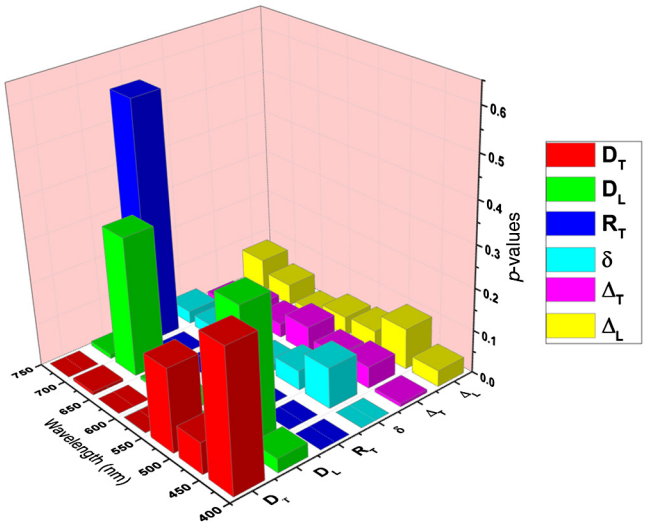

Fig. 9 *P* values obtained from Wilcoxon rank sum test for all six polarimetric properties at various wavelengths.

SVM provides 100% test accuracy, sensitivity, and specificity, respectively, for four polarization properties including Δ_T, Δ_L, R_T and δ. Contrarily, SVM provided 66.6% test accuracy, 33.3% sensitivity, and 83% specificity for both D_T and D_L. Furthermore, MCC and F-measure were found to be unity for the abovementioned four polarization properties, while for D_T and D_L they were resulted in not-a-number as shown in Table 2. Then, we have combined different polarization properties and applied SVM to each combination. In this case, SVM successfully discriminated the normal and adenocarcinoma colon samples with 100% test accuracy, sensitivity, specificity, and with MCC and *F*-measure were found to be unity. From Table 2, it is obvious that SVM fully categorized (100%) normal and adenocarcinoma colon samples for all kinds of combinations of polarization properties, even when total and linear diattenuations were included in these combinations. The "bad classification" of normal and adenocarcinoma colon tissue samples by SVM for total and linear diattenuations may be attributed to the overlapping of error bars for these polarization properties. Overall, we conclude that the better performance of SVM provided the confidence in the classification methodology we have acquired for the detection of normal and adenocarcinoma human colon tissue samples.

Table 2 Support vector machine (SVM)-based classification of normal and cancerous colon tissue samples.

Property	Accuracy (%)	Sensitivity (%)	Specificity (%)	MCC	*F* measure
Δ_T	100	100	100	1	1
Δ_L	100	100	100	1	1
D_T	66.6	33.3	83.3	NAN[a]	NAN
D_L	66.6	33.3	83.3	NAN	NAN
R	100	100	100	1	1
δ	100	100	100	1	1
Δ_T, Δ_L	100	100	100	1	1
Δ_T, Δ_L, D_T	100	100	100	1	1
$\Delta_T, \Delta_L, D_T, D_L$	100	100	100	1	1
$\Delta_T, \Delta_L, D_T, D_L, R$	100	100	100	1	1
$\Delta_T, \Delta_L, D_T, D_L, R, \delta$	100	100	100	1	1

[a]NAN stands for not a number.

4 Conclusion

We have exploited polarized light for the differentiation of *ex vivo* normal and adenocarcinoma human colon tissue samples in the visible spectral range (425–725 nm). Histopathological slides were prepared from 24 human colon tissues including normal and adenocarcinoma samples for both pathology and polarimetry studies. Mueller matrix analysis along with polar decomposition method was employed for extraction and analysis of polarization metrics.inline-formula Our results show that the extracted polarization properties, namely Δ_T, Δ_L, D_T, D_L, R_T, and δ, for adenocarcinoma colon tissue samples were significantly higher compared to the normal colon tissue samples. The performance of the detection method was further assessed by Wilcoxon rank sum test and SVM. Wilcoxon rank sum test illustrated that retardance and depolarization are good candidates for the discrimination of normal and adenocarcinoma colon samples. Moreover, SVM classifier showed a better performance for distinguishing normal and adenocarcinoma colon samples for all polarization properties except D_T and D_L. Our results show that SVM provided 100% accuracy, sensitivity, and specificity for Δ_T, Δ_L, R_T and, δ individually as well as for any combination of above mentioned six polarization properties.

Acknowledgments

Professor Dr. Anwar (Anwar Clinical Laboratory, Swat, Pakistan) is gratefully acknowledged for providing us with *ex vivo* colon tissue samples and his valuable histopathological opinion. This work was supported by IT Endowment and Telecom Fund, PIEAS, Pakistan.

References

1. X. Shao, W. Zheng, and Z. Huang, "In vivo diagnosis of colonic precancer and cancer using near-infrared autofluorescence spectroscopy and biochemical modeling," *J. Biomed. Opt.* **16**(6), 067005 (2011).
2. A. Jemal et al., "Cancer statistics," *CA. Cancer J. Clin.* **59**(4), 225–249 (2009).
3. F. Jenkinson and R. J. C. Steele, "Colorectal cancer screening - methodology," *Surgeon* **8**(3), 164–171 (2010).
4. R. S. Gurjar et al., "Imaging human epithelial properties with polarized light-scattering spectroscopy," *Nat. Med.* **7**(11), 1245–1248 (2001).
5. Y. Zhao, L. Zhang, and Q. Pan, "Spectropolarimetric imaging for pathological analysis of skin," *Appl. Opt.* **48**(10), D236–D246 (2009).
6. M. F. G. Wood et al., "Proof-of-principle demonstration of a Mueller matrix decomposition method for polarized light tissue characterization in vivo," *J. Biomed. Opt.* **14**(1), 014029 (2009).
7. S. L. Jacques, J. C. Ramella-Roman, and K. Lee, "Imaging skin pathology with polarized light," *J. Biomed. Opt.* **7**(3), 329–340 (2002).
8. J. Chung et al., "Use of polar decomposition for the diagnosis of oral precancer," *Appl. Opt.* **46**(15), 3038–3045 (2007).
9. P. Shukla and A. Pradhan, "Mueller decomposition images for cervical tissue: potential for discriminating normal and dysplastic states," *Opt. Express* **17**(3), 1600–1609 (2009).

10. M. Ahmad et al., "Ex vivo assessment of carbon tetrachloride (CCl(4))-induced chronic injury using polarized light spectroscopy," *Appl. Spectrosc.* **67**(12), 1382–1389 (2013).
11. L. Martin et al., "Mueller matrix three-dimensional directional imaging of collagen fibers Mueller matrix three-dimensional directional imaging of collagen fibers," *J. Biomed. Opt.* **19**(2), 026002 (2014).
12. A. Pierangelo et al., "Polarimetric imaging of uterine cervix: a case study," *Opt. Express* **21**(12), 281–289 (2013).
13. N. Ghosh et al., "Mueller matrix decomposition for polarized light: assessment of biological tissues," *J. Biophotonics.* **2**(3), 145–156 (2009).
14. W. Wang et al., "Roles of linear and circular polarization properties and effect of wavelength choice on differentiation between ex vivo normal and cancerous gastric samples," *J. Biomed. Opt.* **19**(4), 046020 (2014).
15. A. Pierangelo et al., "Ex-vivo characterization of human colon cancer by Mueller polarimetric imaging," *Opt. Express* **19**(2), 1582–1593 (2011).
16. A. Pierangelo et al., "Ex vivo photometric and polarimetric multilayer characterization of human healthy colon by multispectral Mueller imaging," *J. Biomed. Opt.* **17**(6), 066009 (2012).
17. D. Hidović-Rowe and E. Claridge, "Modelling and validation of spectral reflectance for the colon," *Phys. Med. Biol.* **50**(6), 1071–1093 (2005).
18. Z. Huang et al., "Laser-induced autofluorescence microscopy of normal and tumor human colonic tissue," *Int. J. Oncol.* **24**(1), 59–63 (2004).
19. M. Antonelli et al., "Impact of model parameters on Monte Carlo simulations of backscattering Mueller matrix images of colon tissue," *Biomed. Opt. Express.* **2**(7), 1836–1851 (2011).
20. R. Siegel, C. Desantis, and A. Jemal, "Colorectal cancer statistics," *CA. Cancer J. Clin.* **64**(2), 104–117 (2014).
21. S.-Y. Lu and R. A. Chipman, "Interpretation of Mueller matrices based on polar decomposition," *J. Opt. Soc. Am. A* **13**(5), 1106 (1996).
22. J. Morio and F. Goudail, "Influence of the order of diattenuator, retarder, and polarizer in polar decomposition of Mueller matrices," *Opt. Lett.* **29**(19), 2234–2236 (2004).
23. B. H. Ibrahim et al., "Determination of collagen fiber orientation in histological slides using Mueller microscopy and validation by second harmonic generation imaging," *Opt. Express* **22**(19), 430–442 (2014).
24. S. Kumar et al., "Comparative study of differential matrix and extended polar decomposition formalisms for polarimetric characterization of complex tissue-like turbid media," *J. Biomed. Opt.* **17**(10), 105006 (2012).
25. B. Zhou et al., "Polarization imaging for breast cancer diagnosis using texture analysis and SVM," in *Proc. IEEE/NIH Life Science Sysytems Applications Workshop (LISSA 2007)*, pp. 217–220 (2008).
26. R. Cicchi et al., "From molecular structure to tissue architecture: collagen organization probed by SHG microscopy," *J. Biophotonics* **6**(2), 129–142 (2013).
27. D. Arifler et al., "Light scattering from collagen fiber networks: micro-optical properties of normal and neoplastic stroma," *Biophys. J.* **92**(9), 3260–3274 (2007).
28. K. Sokolov et al., "Reflectance spectroscopy with polarized light: is it sensitive to cellular and nuclear morphology," *Opt. Express* **5**(13), 302 (1999).
29. C.-C. Yu et al., "Assessing epithelial cell nuclear morphology by using azimuthal light scattering spectroscopy," *Opt. Lett.* **31**(21), 3119 (2006).
30. M. Hilska et al., "The distribution of collagen types I, III, and IV in normal and malignant colorectal mucosa," *Eur. J. Surg.* **164**(6), 457–464 (1998).
31. Y. Furuya and T. Ogata, "Scanning electron microscopic study of the collagen networks of the normal mucosa, hyperplastic polyps, tubular adenoma, and adenocarcinoma of the human large intestine," *Tohoku J. Exp. Med.* **169**(1), 1–19 (1993).
32. J. Turnay et al., "Collagen metabolism in human colon adenocarcinoma," *Connect. Tissue Res.* **23**(4), 251–260 (1989).
33. M. K. Swami et al., "Polar decomposition of 3×3 Mueller matrix: a tool for quantitative tissue polarimetry," *Opt. Express* **14**(20), 9324–9337 (2006).
34. M.-R. Antonelli et al., "Mueller matrix imaging of human colon tissue for cancer diagnostics: how Monte Carlo modeling can help in the interpretation of experimental data," *Opt. Express* **18**(10), 10200–10208 (2010).
35. J. A. K. Suykens and J. Vandewalle, "Least squares support vector machine classifiers," *Neural Process. Lett.* **9**(3), 293–300 (1999).

Iftikhar Ahmad received his MSc degree in medical physics from PIEAS, Pakistan, in 2007. Currently he is pursuing his PhD studies. He is the recipient of IT and EF postgraduate scholarship and an exchange program scholarship for the University of Toronto. His work focuses on the polarimetric characterization of biological tissues. This is his third first-author publication.

Manzoor Ahmad has been working as an assistant professor at the Department of Physics, Islamia College (University), Peshawar. He completed his PhD from Pakistan Institute of Engineering and Applied Sciences (PIEAS) in 2014 under an indigenous scholarship sponsored by the higher education commission of Pakistan. He used polarized light for tissue characterization during his research. His research interests include polarized light imaging, elastic light scattering, diffuse reflectance, and Monte Carlo modeling of light propagation through tissues.

Karim Khan received his MS degree in medical physics from PIEAS University Islamabad, Pakistan, in 2007. He is working as a senior scientist in SINOR Cancer Hospital Swat. Currently, he is doing his PhD in the field of biophotonics at PEAS. His main field of interest is tissue polarimetry.

Sumara Ashraf is pursuing her PhD in the field of biomedical optics and polarimetry at PIEAS, Pakistan. She is the recipient of "Indigenous PhD Scholarship, Pakistan" and an exchange program scholarship for the University of Toronto. She worked as part of Dr. Alex Vitkin's Laboratory on noninvasive glucose monitoring using polarized light.

Shakil Ahmad received his MS degree in nuclear medicine from PIEAS in 1997. He is working as the director of SINOR Cancer Hospital, Pakistan. His main field of interest is sonography imaging and nuclear imaging.

Masroor Ikram received his MSc degree in physics from Quaid-i-Azam University, Islamabad, Pakistan, and his PhD in laser physics from the University of Cambridge, Cambridge, UK, in 1990. Currently, he is the professor of physics and director (academics) of the Pakistan Institute of Engineering and Applied Sciences, Islamabad, Pakistan. His main research area is biophotonics, which include biomaterials, optical imaging, polarimetry, and photodynamic therapy.